Acta Geodyn. Geomater., Vol. 7, No. 2 (158), 145–152, 2010

STRUCTURE AND PERMEABILITY OF DEEP-SEATED ROCKS IN THE KOLA SUPERDEEP BOREHOLE SECTION (SG-3)

Felix F. GORBATSEVICH [1)] *, Serafim V. IKORSKY [1)] and Andrey V. ZHARIKOV [2)]

[1)] Geological Institute of the Kola Science Centre RAS, Apatity
[2)] Institute of Geology of Ore Deposits, Petrography, Mineralogy and Geochemistry, RAS, Moscow
**Corresponding author's e-mail:* gorich@geoksc.apatity.ru

(*Received* August 2009, *accepted* December 2009)

ABSTRACT
Preferential flow paths in the crust, as caused by the presence of the Luchlompolo fault in the drilled section of the Kola Superdeep Borehole (SG-3) and the dip angle of the rock structural elements (layering, schistosity, banding), are favourable for migration of deep fluids to the Earth's surface. An investigation of the structure, anisotropy and permeability of rocks under PT-conditions in the SG-3 section, in addition to the occurrence of He-isotopes, reveals that the high-permeability zones of the exposed crustal segment are related to two important structural elements of the section: in the upper zone – to the Luchlompolo fault, in the lower one to the contact between the Proterozoic and Archaean complexes. The obtained results on the rock samples from SG-3 indicate a rough correlation between permeability and elastic anisotropy of various rock samples. Simulating increased PT-conditions, corresponding to the relevant depths of 6-8 km document the overlapping temperature and pressure effect, i.e. resulting in a sharp decrease of rock permeability.

KEYWORDS: crystalline crust, permeability, anisotropy, rocks, structure, helium

INTRODUCTION

The in-situ permeability of deep-seated crystalline rocks of the continental crust and the infiltration degree of various fluids through these rocks are of great theoretical and practical importance. Only few scientific wells recently drilled into the basement and metamorphic rocks provide insight in the permeability structure of the crust. Because scale effects are obvious various kinds of permeability methods have to be applied. Among these methods are various types of laboratory tests, observations on the fluids entering boreholes, ways of pressure injection of liquid into the isolated part of a borehole, recording of the deep fluid migration through cracks and faults etc. (Bayuk et al., 1987; Clauser, 1992; Huenges et al., 1997; Zimmermann et al., 2000).

Aiming on larger scales, i.e. the borehole scale, one of the fluid transportation markers may be the mantle gas ^{3}He (Orlov and Laverov, 1998). In the smaller scale, there are various experimental methods available to measure rock permeability on core samples recovered from drill holes at corresponding PT-parameters under lab conditions. Due to the complexity of lithology and structural elements of the crystalline crust, only an integrated study of the relation between a rock structural, material and physical parameters and flow intensity of deep gases enables one to reveal the characteristic features of zones with increased permeability and fluid incurrent channels to the Earth's surface etc.

The Kola Superdeep Borehole (SG-3) that holds the record for the depth of penetration into the Earth's crust is the most favourable object for investigations of permeability of deep crystalline rocks (Kozlovsky, 1987; Orlov and Laverov, 1998). The borehole was drilled in the north-western Kola Peninsula within the Pechenga graben-syncline. Down to a depth of 6842 m the SG-3 section is represented by sedimentary-volcanic rocks of the Lower Proterozoic Pechenga complex, below gneisses and amphibolites of the Archaean basement occur. A large body of new results of various investigations was obtained at the Kola Superdeep Borehole. Among them the data on petrophysical properties of deep rocks, their comparison with the properties of surface rocks are of great interest (Kern et al., 2001; Trčková et al., 2002). The SG-3 unique depth allowed an assessment of rock porosity and permeability to be made not only in a sample but on the scale of the entire borehole. The task was alleviated by the fact that at a depth of 4673 m the borehole intersects the Luchlompolo fault through which, as it was found, noble gases (their isotopes) enter the borehole experimental data sets focusing on the permeability and velocity structure of the SG-3 section which allows not only correlations between the various parameters but also identification of the prominent fluid pathways in this crustal segment which may the reason for increased ^{3}H/^{4}He ratios.

THE STRUCTURE OF THE SG-3 SECTION

Four facies of regional metamorphism – from prehnite-pumpellyite to amphibolite (below 6 km) were identified in the section from top to bottom. According to isotopic dating the age of sedimentation and volcanism of the Pechenga complex is 2.4-1.9 Ga, the age of metamorphism - 1.9-1.7 Ga (Orlov and Laverov, 1998; Bayanova et al., 2002). The U-Pb and Pb-Pb zircon age of ancient metamorphism of the Archaean complex is 2.9-2.8 Ga.

An analysis of the beds spatial location made by instrumental methods within the SG-3 Proterozoic and Archaean sections shows that the inclination of the structural elements (layering, schistosity, banding) about the borehole axis ranges from 40^o to 60^o, Figure 1. In the Figure the dip of the litho-structural elements, e.g. bedding, is indicated by an angle γ. The angle α was determined by the acoustopolariscopy method (Gorbatsevich, 1995). Both angles were measured in relation to the axis of the core (borehole). The angle α represents the spatial location of the elastic anisotropy plane in the core samples.

The Figure 1 also shows the measured spatial location of these elements (solid line) within every formation and unit. Within the whole section three large intervals in which the angle γ values are held can be identified. The first interval is down to a depth of ~ 4.0 km. In this range the prevailing angle γ values are $40\text{-}50^o$. At depths of ~1.1 and ~2.0 km the variations of the angle γ are much wider – from 10^o to 50^o and from 4^o to 70^o accordingly. Below 4.4 km down to a depth of 7 km the average value of the angle γ is $\sim 70^o$. At a depth of 7.0-8.4 km a smooth fall of the angle γ to $40\text{-}50^o$ is observed. These values are also typical of the 8.4-11.5 km depths.

Figure 1 allows one to note that within the Luchlompolo fault the angle γ varies from 40^o to 75^o. The angle α shows even greater variations (Sharov, 1997). At a depth of 4.4-4.7 km a rather remarkable fact is observed – the angle α passes virtually the whole spectre of possible values in the range of $0\text{-}90^o$. Such changes in the spatial location of the elastic anisotropy plane can signify that at these depths a shearing stress with a possible displacement of some beds and members occurred. Down to a depth of 4.4 km the values of the angles α and γ are more or less constant and below 4.7 km they increase about twice. Since rocks at a depth of 4.4-4.7 km are in the Luchlompolo fault zone, it is believed that the change in the average angles α and γ above and below the fault is caused by a displacement of the overlying block in relation to the underlying one (Kazansky et al., 1994).

Visual and microstructural investigations also point to the existence of the border between different structural stages and to the peculiarities of the processes related to the Luchlompolo fault formation. Shearing and mylonization of rocks are typical of the fault zone (Kozlovsky, 1987). A structural-textural analysis showed that schistosity developed in the tectonized areas of the Luchlompolo fault as well as blastomylonite and blastocataclasite from tectonic sutures possess a clear and uniform mineral orientation. Optical axes of quartz in rocks are oriented by the R-tectonite and S-tectonite "flattering" type. Biotite flakes are oriented by the S-tectonite type with one maximum perpendicular to schistosity. S-tectonites are rocks in which optical axes of quartz are parallel. Such arrangement of axes points to the

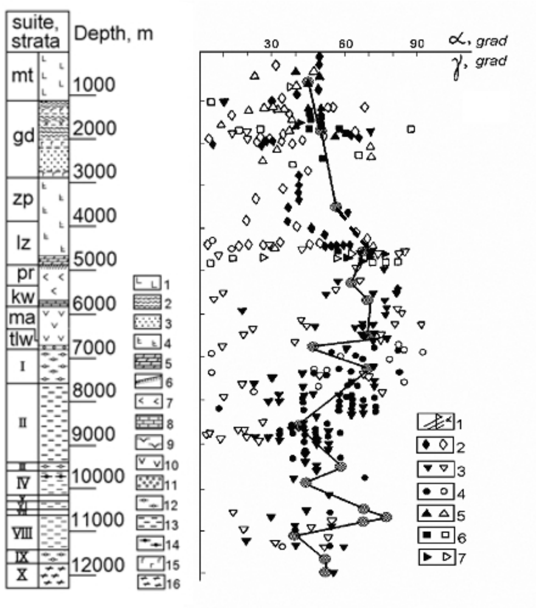

Fig. 1 Distribution of the rock structural elements in the Kola Superdeep Borehole section.

1 – augitic metadiabase with pyroxene and picrite porphyrite interbeds; 2 – metaphyllite, metasiltstone with metatuff interbeds; 3 – rhythmically alternating metasandstone with subordinate metasiltstone and metaphyllite; 4 – actinolized metabasalt; 5 – dolomite, arkose metasandstone; 6 – sericitic schist; 7 – metabasalt; 8 – dolomite, polimictic metasandstone; 9 – vehrlite; 10 – metaporphyrite, schist after it; 11 – metasandstone; 12 – biotite-plagioclase-gneiss with high-alumina minerals; 13 - biotite-plagioclase-gneiss with amphibole, epidote, sphene; 14 – magnetite-amphibole schist; 15 – gabbro-diabase; 16 – biotite-plagioclase and sphene-biotite-amphibole-plagioclase gneiss, schist.

mt – Matert, gd – Zhdanov, zp – Zapolyarny, lz – Luchlompolo, pr – Pirttijarvi, kw – Kuvernerinjoki, ma – Majarvi, tlw – Televi Fms.

I – X – units in the Archaean section.

Measured spatial location of the structural elements (bedding, schistosity, banding) is shown as solid line. Unit values of angles a - between the plane of rock elastic anisotropy and the borehole axis and angle γ – schistosity (bedding, banding) about the same axis are shown as dots, triangles, etc.

1 – sketch for calculating angles α and γ; 2 – metabasalts; 3 – amphibolite, peridotite, schist; 4 – gneiss, granite, migmatite; 5 – metaphyllite, metatuff; 6 – metasandstone, metasiltstone; 7 – metaporphyrite.

existence of conditions for translation gliding. It is noteworthy that during the seismic survey preceding the borehole location, an inclined boundary between the Proterozoic and Archaean complexes was drawn along the Luchlompolo fault and the real contact between these complexes was interpreted as the boundary between gneisses and underlying rocks of the granulite-basalt layer (Kozlovsky, 1987). In this zone of the borehole a rapid increase in the borehole cavernosity and a local rise in gases and water inflow were observed.

Seismic sounding, in particular vertical seismic profiling with shear waves, also showed the presence of a boundary between rather homogeneous and anisotropic rocks (Digranes et al., 1996). Below this boundary the polarization vector of shear waves takes on a distinct direction. A great difference in the degree of rock anisotropy at this boundary together with the influence of velocity gradients and temperature can cause seismic reflections registered at the Earth's surface (Christensen, 1985; Burtny et al., 1991). In our opinion, the boundary at a depth of ~4.5 km is tectonic and it does not fully coincide with the lithological boundary between the third volcanic and the third tuffaceous-sedimentary suites. It is the boundary separating virtually isotropic rocks from highly anisotropic ones (Il'chenko et al., 2005).

OCCURRENCE OF HE-ISOTOPES – INDICATOR OF LARGE SCALE FLUID TRANSPORT FROM THE MANTLE INTO THE CRUST

The Luchlompolo fault can be a conducting zone for deep including mantle gases as may be indicated by different helium isotope abundances and $^3He/^4He$ ratios, measured in the samples from the entire SG-3 section (Ikorsky et al., 1994). The investigation was performed in two steps:

1. At the first stage most attention was concentrated on the Archaean rocks and rock forming amphiboles, because the obtained results represent the background of a crustal segment unaffected by fluid interactions from the mantle.
2. The study of the helium isotope distribution in the borehole section allows one to see whether the $^3He/^4He$ ratio established for the Precambrian platforms (on the average $1.8{\cdot}10^{-8}$) is kept or it will increase as the boundary with the upper mantle is approached. The present-day $^3He/^4He$ ratios for the upper mantle are taken equal to $1.2{\cdot}10^{-5}$ (Shukolyukov, 1983; Tolstikhin, 1986).

The study of the helium isotope distribution within the Karelian complex was conducted on a limited number of metadiabase samples representing four Proterozoic volcanic formations. Helium emission was performed by sample melting (Mitrofanov, 1991). Helium was also extracted by sample crushing in sealed vacuum glass ampoules. The principle of crushing in ampoules is outlined in (Ikorsky and Kushch, 1992). Unlike melting when the entire helium is extracted, in the course of crushing He is liberated from fluid inclusions of microscopic size. Besides rocks, quartz samples from synmetamorphogenetic veins of the Pechenga complex and from veins and pegmatite of the Archaean complex were studied. As a rule, samples from quartz veins were accompanied by home rock specimens taken at a distance of 0.5-3 cm from the contact with the vein. An analysis of the helium isotopic composition was performed in a mass-spectrometer MI-1201 No. 22-78. The ampoules with crushed samples were opened in a breaking device connected with the lap system of the mass-spectrometer.

The procedure testing showed that the measured $^3He/^4He$ ratios are independent of the completeness of helium extraction from the samples. The $^3He/^4He$ ratios obtained by melting and crushing at equal depths are virtually the same. The amount of ^4He extracted by crushing is, on the average, 5 % for metadiabase, 25 % for gneiss and 4% for amphibolite of its total content determined by melting. The greatest amount of ^4He extracted by melting was (x 10^{-6} cm^3/g): 860 in metadiabase, 670 in gneiss, and 1760 in amphibolite (Ikorsky et al., 1994). The greatest amount of ^4He extracted by crushing was in quartz from the tourmaline-quartz veinlet in the andesite porphyrite of the Luchlompolo Fm at a depth of 4763.1 m. Step-wise annealing (3-10 temperature steps) performed on three samples of rock forming amphibole with the ratio of $^3He/^4He \approx 1{\cdot}10^{-9}$ showed that the results obtained are independent of the annealing temperature (within 360-1000 °C). The measured $^3He/^4He$ ratios through the entire SG-3 section are given in Figure 2a.

It is worth noting that for the upper mantle the modern $^3He/^4He$ ratio is taken equal to $1.2{\cdot}10^{-5}$, whereas for the typical radiogenic helium of the crust - $\sim 2{\cdot}10^{-8}$ (Shukolyukov, 1983). Figure 2a shows that intervals or zones with radiogenic or near-radiogenic $^3He/^4He$ ratios alternate with zones where these ratios are 5-6 times greater than radiogenic crustal values. Within every zone all rocks independent of their composition and genesis as well as quartz from synmetamorphogenic veins have different helium abundances but virtually equal $^3He/^4He$ ratios.

From the surface down to a depth of 2.8 km the $^3He/^4He$ ratio corresponds to the radiogenic crustal level and is in the range of $1.8{\cdot}10^{-8}$ - $4.1{\cdot}10^{-8}$ with prevailing values of $(1.8\text{-}2.2){\cdot}10^{-8}$. This zone covers the whole section of the Matert volcanic and Zhdanov sedimentary Fms. Below the $^3He/^4He$ ratio rapidly increases and in the 3.2-5.7 km range it is $(10\text{-}13){\cdot}10^{-8}$. These values are typical of both igneous (metadiabase, metaandesite, metaalbitophyre) and metasedimentary (arkose sandstone, limestone) rocks from the Proterozoic Zapolyarny, Luchlompolo, Pirttijarvi and Kuvernerinjoki Fms and also of synmetamorphogenic veins developed in these

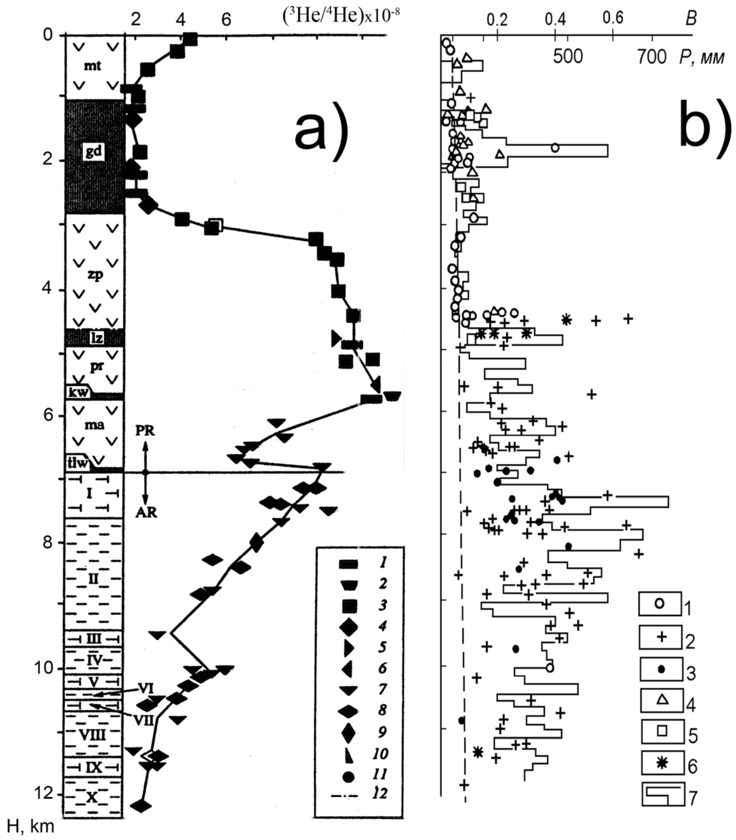

Fig. 2 Distribution of the $^3He/^4He$ ratio; unit values of elastic anisotropy *B* and cavernosity *P* of rocks in the Kola Superdeep Borehole section.

a – distribution of the $^3He/^4He$ ratio in the Kola Superdeep Borehole section. Rock types from which the samples were taken to determine $^3He/^4He$ are designated by numbers.

1 – metaphyllite, metasiltstone, metasandstone; 2 – metalimestone; 3 – metadiabase; 4 – gabbro-diabase; 5 – andesite metaporphyrite; 6 – metaalbitophyre; 7 – amphibole schist and amphibolite; 8 – gneiss; 9 – aplite; 10 – amphibole from amphibolite; 11 – quartz from synmetamorphogenic veins and pegmatite; 12 – location of the Luchlompolo fault.

b – anisotropy index *B*.

1 – metadiabase, peridotite; 2 – amphibolite, schist; 3 – gneiss, granite, migmatite; 4 – metaphyllite, metatuff; 5 – metasandstone, metasiltstone; 6 – metaporphyrite; 7 – average interval lateral dimension *P* of the borehole.

An analysis of Figure 2a shows that in the borehole two zones can be distinguished in which the $^3H/^4He$ ratio is several times greater than the radiogenic values typical of the rest section. The upper zone is located in the Proterozoic sedimentary-volcanic rocks in the range of 3.2–5.7 km, the lower one – at a depth of 6.8–7.5 km and includes the lowermost strata of the Pechenga complex and the upper Archaean complex. These zones of increased $^3He/^4He$ ratios are related to two important structural elements of the section: the upper zone - to the Luchlompolo fault, the lower one - to the contact between the Proterozoic and Archaean complexes. In our view, a relative enrichment of helium in ^3He in these zones can be explained by the fact that the Luchlompolo formations; they bear witness to the presence of up to 1 % of the mantle component in He.

Below in the range of 6-6.7 km in shaly amphibolite of the Majarvi Fm the $^3He/^4He$ ratio decreases to $6 \cdot 10^{-8}$ and then again increases to $10 \cdot 10^{-8}$ in shaly amphibolite of the Majarvi Fm basement, gneiss and amphibolite of the upper Archaean complex in the range of 6.8-7.5 km. Deeper the $^3He/^4He$ ratio gradually decreases and takes typical radiogenic values at a depth of about 10.5 km. This distribution of helium isotopes in the Archaean section is typical of not only the main rock varieties – gneiss and amphibolite but also of monomineral fractions of rock forming amphibole and quartz from veins and pegmatite (Fig. 2a).

fault acts as a channel through which the mantle helium enters the upper crustal rocks. The Luchlompolo fault which effects (in terms of dislocation metamorphism) are traced up and down the section at great distances, together with the contact between the Proterozoic and Archaean complexes where tectonic shoves occurred, were conducting zones for fluids carrying helium with the mantle component. This gas is infiltrated through a developed fracture network above and below the fault. The greatest positive anomaly of the heat flow - to 65 mW m^2 is confined to the Luchlompolo fault which is likely to be caused by fluid motion along the fault (Orlov and Laverov, 1998).

ELASTIC ROCK ANISOTROPY AS INDICATOR FOR POTENTIAL FLUID PATH-WAYS

As a laboratory approach the presence of the 6.8–7.5 km permeable zone is related to the measured elastic anisotropy on dilated cores. In the past it was demonstrated that at this interval fracturing and rock anisotropy – both structural and elastic - are most conspicuous (Sharov et al., 2005). This is indicated by the determined elastic anisotropy obtained on a large number of the core samples from SG-3, Figure 2b. Anisotropy indexes *B* (Fig. 2b) were studied on the samples by the acoustopolariscopy method in laboratory conditions at barometric pressure and temperature (Gorbatsevich, 2009). In accordance with this method, first the location of elastic symmetry element projections was determined on the three pairs of faces of a deep sample. Then compression wave velocities were measured on all the pairs of faces and in accordance with the revealed symmetry element projections, shear wave velocities were determined. The index *B* was calculated from the measured shear wave velocities (Gorbatsevich and Smirnov, 2000).

The distribution of the values *B*, Figure 2b, as well as the results of the structural-textural analysis gives grounds to distinguish two parts of the section that differ greatly in anisotropy. The first one from the surface down to a depth of 4.43 km contains weakly anisotropic and virtually isotropic rocks, such as metadiabase, peridotite, metaphyllite, metatuff, metasandstone and metasiltstone. Within the first part the mean value of index $B = 0.08$. In the 1.8–2.1 km interval there is a section with highly anisotropic rocks where interlayers of copper-nickel mineralization were observed (Kozlovsky, 1987). A sharp boundary ($H = 4.43$ km) dividing the two parts by the factor of elastic anisotropy passes in the Luchlompolo fault area. Rocks occurring below 4.43 km (mainly amphibolite, schist, gneiss, granite and migmatite), on the average, are strongly anisotropic. At some intervals index $B > 0.4$. In the range of 4.56 to 4.88 km under the action of anisotropy of elastic-strength properties a dogleg of the borehole takes place with transition from an angle of 4° 25' to 7° 20' between the borehole axis and the vertical. The areas with the highest anisotropy were registered at the 4.43-4.95, 5.75-7.0 and 7.4-8.65 km depths. Judging by the maximum values of *B*, below 8.3 km elastic anisotropy of rocks decreases monotonically.

It should be noted that through the entire borehole section there is an evident correlation between the maximum index *B* and the cavern size *P* (maximum diameter) in the borehole (Gorbatsevich et al., 1997). For instance, in the range of $H = 1.7$-1.9 km where the average cavern size is $P = 0.58$ m, rocks with high values of $B = 0.39$ were observed. In rocks with $B = 0.64$ occurring at a depth of 4.55 km and below an increase of caverns to $P = 0.41$-0.47 m was observed. At a depth of 7.4-8.3 km with the highest $B = 0.56$-0.67 in the section the cavern size reached P = 0.72 m. From a depth of 8.3 km and below the values of *B* and *P* decrease monotonically.

The correlation between the values of *B* and *P* is explained by the fact that elastic anisotropy of rocks is related to so-called mechanical anisotropy or strength anisotropy. The strength anisotropy as well as elastic anisotropy of rocks is affected by weakening surfaces including contacts between elongated grains of different minerals, cleavage planes (biotite, muscovite etc.), microcracks, systemic jointing, structural elements of layering, schistosity and banding. It is precisely along the mentioned weakening surfaces that fluid transport is possible for comparatively long distances. If we compare the $^3He/^4He$ ratio trends and elastic anisotropy index *B* along the SG-3 section, Figs. 2a and 2b, we can observe the trend coincidence of these parameters for some depth intervals.

First of all, starting with the Proterozoic-Archaean boundary a simultaneous decrease in the $^3He/^4He$ ratio and index *B* with depth takes place. From the Proterozoic-Archaean boundary to the Luchlompolo Fm (fault) the values of the $^3He/^4He$ ratio and *B* remain high. In the range of 3.1-4.4 km with rather high $^3He/^4He$ ratios, the values of *B* indicate weak anisotropy of rocks. Such a difference can imply that there is a systemic jointing over this interval able to transport easily penetrating gases ^3He and ^4He. In the range of 1.7-1.9 km members of highly anisotropic rocks occur. However the $^3He/^4He$ ratio in a sample from this range is near-radiogenic. This indicates that this interval has no fluid incurrent channels from the Luchlompolo fault.

Figure 2a allows one to note that the $^3He/^4He$ ratio does not increase with depth. The increase of this index observed in the middle section can be explained by increased permeability of rocks in the Luchlompolo fault zone. In this connection, natural permeability of dense rocks in the SG-3 section is of interest. By now there is a rather small body of data that enables one to trace some general trends from modelling PT-conditions and the change in permeability of rock samples from superdeep boreholes with depth.

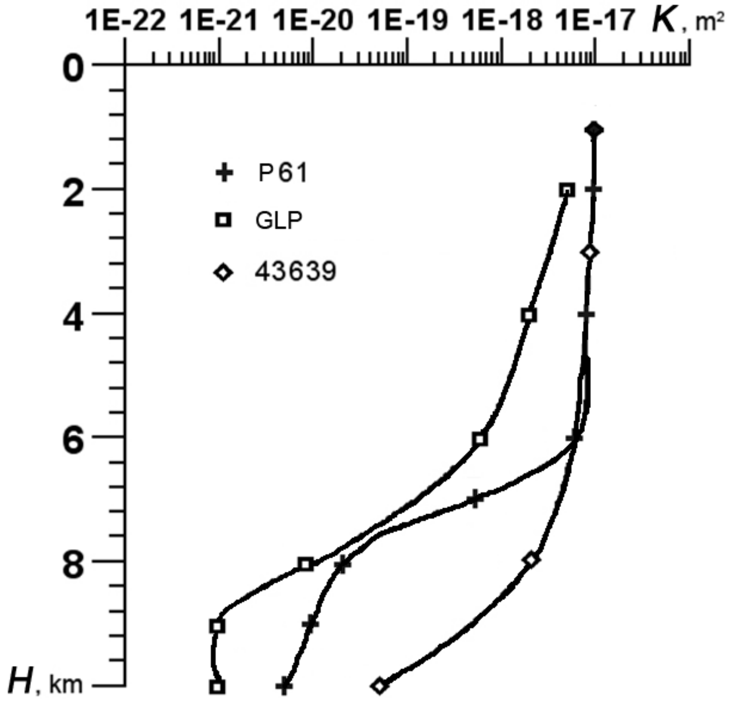

Fig. 3 Dependences of permeability of amphibolite samples from the Earth's surface (P61), 3847 m (GLP) and 11400 m depths (43639) at simultaneous loading and heating imitating depth increase in the SG-3 section.

PERMEABILITY AT PT-CONDITIONS

To provide a direct insight in the permeability structure of the crust permeability *K* was measured on a small scale on drill cores in the laboratory (mostly under simulated in situ pressures). As an example, Figure 3 shows dependences of permeability of samples produced from the SG-3 core and their surface analogues obtained at simultaneous loading and heating imitating depth increase (Zharikov et al., 2000). In the experiment amphibolite samples from the Earth's surface (P61), 3847 m (GLP) and 11400 m (43639) epths were used. As the plot suggests, a depth increase causes a decrease in permeability *K* in all samples. The permeability decreases with a variously changing gradient – at a depth of 6-8 km one can see a conspicuous s-shaped bend on the plot. At the same depths one can see the greatest discrepancy in *K* values. As the temperature and pressure increase to the values corresponding to the PT-parameters at a depth of 10 km, these discrepancies decrease to the values comparable with the measurement error.

A comparison of the obtained trends with theoretical dependences and microstructural study data suggests that such permeability behaviour is caused by transition from fissure to block permeability resulting from a change of a brittle deformation style to a more plastic one (Zharikov et al., 2000).

There is a vast summary of data sets combining the results of long-standing investigations of rock permeability in laboratory conditions, observations made in boreholes and on regional scales (Clauser, 1992). A comparison of our data with those published shows that the sample permeability, Figure 3, obtained under simulated conditions corresponding to a depth of 1-2 km is ~10^{-17} m^2. This value is somewhere in the middle of the range of the published summary of results. At the same time the data corresponding to a depth of 10 km, are closer to extreme values ($K = 10^{-19} - 10^{-21}$ m^2, Fig. 3) of the value range of rock permeability presented in (Clauser, 1992). After Clauser, the permeability of massifs which thickness is comparable with the borehole depth is in the range of $K = 10^{-12}$-10^{-21} m^2.

CONCLUSION

The Luchlompolo fault in the drilled section of the Kola Superdeep Borehole (SG-3) and the dip angle of the rock structural elements (layering, schistosity, banding) were identified as potential pathways for migration of deep fluids from the upper mantle to the Earth's surface as indicated by fluid compositions with the mantle component admixture (^3He).

Two zones were distinguished in which the $^3H/^4He$ ratios are several times higher than radiogenic values typical for the rest part of the section. The upper zone is located in Proterozoic sedimentary-volcanic rocks in the range of 3.2–5.7 km, the lower zone – at a depth of 6.8–7.5 km. The latter one includes the lowermost strata of the Pechenga complex and the upper part of the Archaean section. These zones with increased $^3He/^4He$ ratios are confined to two important structural elements of the section: the upper zone – to the Luchlompolo fault, the lower – to the contact between the Proterozoic and Archaean complexes. The mantle gas ^3He is infiltrated directly from the fault zone (~ 4.5 km) to the overlying layers most likely through the systemic jointing.

The high $^3He/^4He$ ratio in the ranges of 4.4–4.8 and 6.8–7.5 km is correlated with the increased rock anisotropy, resulting both from structural and elastic rock properties. The structural elements (layering, schistosity and banding) and elongated rock grain boundaries are attributed to act as pathways that provide fluid transport for long distances. A decrease in the $^3He/^4He$ ratio was observed below the Proterozoic-Archaean contact. Rock elastic anisotropy indicates the same trend. Thus, our results verify the model data that anisotropy of metamorphic rock properties can play an important part in fluid transport (Lyubetskaya and Ague, 2009).

Laboratory measurements of permeability on cores from SG-3 under simulated PT-conditions showed that as the temperature and pressure increase to the values corresponding to the depths of 6-8 km permeability decreases which is attributed to a change from brittle rock deformation to plastic deformation styles thus interrupting conducting pathways. On the whole, the established increase in the $^3He/^4He$ ratio in the middle section is explained by the effect of tectonic factors.

ACKNOLEDGMENT

The work was supported financially by the Russian Foundation for Basic Research, grant № 07-05-00100-a.

REFERENCES

Bayanova, T.B., Pozhilenko, V.I., Smol'kin, V.F., Kudryashov, N.M., Kaulina, T.V. and Vetrin, V.R.: 2002, Catalogue of geochronological data for the north-eastern Baltic Shield. Apatity, KSC RAS, (in Russian).

Bayuk, E.I., Belikov, B.P., Vernik, L.I., Volarovich, M.P., Kuznetsov, Yu.I., Kuzmenkova, G.E., and Pavlova, N.N.: 1987, Rock density, porosity and permeability. The superdeep well of the Kola Peninsula. Kozlovsky, E.A. (ed.). Springer-Verlag. Berlin Heidelberg.

Burtny, P.A., Gorbatsevich, F.F., Ivanov, G.A., Korchin, V.A., Lanev, V.S., Lebedev, T.S., Medvedev, V.V. and Sharov, N.V.: 1991, On the nature of subhorizontal seismic boundaries in the upper crystalline crust of the Baltic Shield. Aspects of multidisciplinary interpretation of geological and geophysical data. Leningrad, Nauka, 122–130, (in Russian).

Christensen, N.I.: 1985, Measurements of dynamic properties of rock at elevated temperatures and pressures. Measurement of rock properties at elevated pressures and temperatures. ASTM STR 869, H.J. Pincus and E.R. Hoskins, (eds.), American Society for Testing and Materials. Philadelphia, 93–107.

Clauser, C.: 1992, Permeability of Crystalline Rocks. EOS Trans. Am. Geophys. Union, 73 (21), 233–237.

Digranes, P., Kristoffersen, Y. and Karajev, N.: 1996, An analysis of shear waves observed in VSP data from the superdeep well at Kola, Russia. Geophys. J. Int., 126, 545–554.

Gorbatsevich, F.F.: 1995, Acoustopolariscopy of rocks. Apatity, KSC RAS, (in Russian).

Gorbatsevich, F.F.: 2009, Acoustopolariscopy of minerals and rocks. VDM Verlag, Saarbrucken.

Gorbatsevich, F.F. and Smirnov, Yu.P.: 2000, Kola Superdeep Borehole: 3D model of elastic anisotropy of crystalline rocks in the upper and middle crust. The results of the study of the deep substance and physical processes in the Kola Superdeep Borehole down to a depth of 12261 m. F.P. Mitrofanov and F.F. Gorbatsevich (eds.). Apatity, Poligraf, 144–148, (in Russian).

Gorbatsevich, F.F., Medvedev, R.V. and Smirnov, Yu.P.: 1997, Elastic-anisotropic properties of the core along the Kola Superdeep Borehole (SG-3). Izv. RAN Ser. Fiz. Zemli, 4, 3–12, (in Russian).

Huenges, E., Erzinger, J., Kück J., Engeser B. and Kessels, W.: 1997, The permeable crust: geohydraulic properties down to 9101 m depth. J .Geophys . Res., 102 (B8), 18255–18265.

Ikorsky, S.V., Kamensky, I.L. and Smirnov, Yu.P.: 1994, Helium isotopes in the Kola Superdeep Borehole section. Doklady AN, 335 (1), 84-87, (in Russian).

Ikorsky, S.V. and Kushch, V.D.: 1992, Nitrogen in fluid inclusions in alkaline rocks of the Khibiny massif and methods of its chromatographic determination. Geokhimiya, 7, 962–970, (in Russian).

Il'chenko, V.L., Gorbatsevich, F.F. and Smirnov, Yu.P.: 2005, Anisotropy of the core elastic properties and the state of the rocks from the near-borehole massif of the Kola Superdeep Borehole in the Luchlompolo fault zone. Geoekologiya. Inzhenernaya Geologiya. Gidrogeologiya. Geokriologiya (3), 1–11, (in Russian).

Kazansky, V.I., Kuznetsov, O.L., Kuznetsov, A.V., Lobanov, K.V. and Cheremisina, E.N.: 1994, Deep structure and geodynamics of the Pechenga ore area: study experience of the Kola Superdeep Borehole. Geologiya Rudnykh mestorozhdeny, 36 (6), 500–519, (in Russian).

Kern, H., Popp, T., Gorbatsevich, F.F., Zharikov, A.V, Lobanov, K.V. and Smirnov, Yu.P.: 2001, Pressure and temperature dependence of Vp and Vs in rocks from the superdeep well and from surface analogues at Kola and the nature of velocity anisotropy. Tectonophysics, 338, 113–134.

Kozlovsky, E.A. (ed.): 1987, The superdeep well of the Kola peninsula. Springer-Verlag. Berlin Heidelberg.

Lyubetskaya, T. and Ague J.J.: 2009, Modeling the Magnitudes and Directions of Regional Metamorphic Fluid Flow in Collisional Orogens, J. Petrology, 50 (8), 1505–1531.

Mitrofanov, F.P. (ed): 1991, Archaean complex in the SG-3 section. Apatity, KSC USSR AS, (in Russian).

Orlov, V.P. and Laverov, N.P. (eds.): 1998, Kola Superdeep. Scientific results and research experience. Moscow, "Technoneftegaz", (in Russian).

Sharov, N.V. (ed.): 1997, Seismological model of Northern Europe lithosphere. Lapland-Pechenga area. Apatity, KSC RAS, (in Russian).

Sharov, N.V., Mitrofanov, F.P., Verba, M.L. and Gillen, C. (eds.): 2005, Lithospheric structure of the Russian Barents region. Petrozavodsk, Karelian SC RAS, 318, (in Russian).

Shukolyukov, Yu.A.: 1983, Geochemistry issues of radiogenic isotopes. Geochemistry, 3, 333–347, (in Russian).

Tolstikhin, I.N.: 1986, Isotopic geochemistry of helium, argon and rare gases. Moscow, Nauka, (in Russian).

Trčková J., Živor R., Kazansky V.I. Lobanov K.V., Zharikov A.V. and Smirnov Y.P.: 2002, Comparison of elastic properties of the Kola Superdeep borehole core samples and their surface analogues obtained by static and dynamic measurements. Acta Montana IRSM AS CR Series A, No. 21 (125), 27–54.

Zharikov, A.V., Vitovtova, V.M. and Shmonov, V.M.: 2000, Permeability of the core samples from superdeep drill holes and their surface analogues at high temperature and pressure. The results of the study of the deep substance and physical processes in the Kola Superdeep Borehole down to a depth of 12261 m. F.P. Mitrofanov and F.F. Gorbatsevich (eds.). Apatity, Poligraf, 110–114, (in Russian).

Zimmermann, G., Körner, A., and Burkhardt, H.: 2000, Hydraulic pathways in the crystalline rock of the KTB. Geophys. J. Int., 142, 4–14.